ANALYTIC MODEL OF LAMINAR-TURBULENT TRANSITION FOR BINGHAM PLASTICS

K. C. Wilson[1*] and A. D. Thomas[2]

1. Queen's University, Department of Civil Engineering, Kingston, ON, Canada K7L 3N6

2. Slurry Systems Pty Ltd., 7 Cantwell Road, Lochinvar NSW 2321, Australia

It is often desirable to operate industrial pipelines transporting non-Newtonian materials near the transition from laminar to turbulent flow. For the commonly used Bingham plastic model, the Hedström technique overestimates turbulent flow friction losses because it does not take account of viscous-layer thickening. In the present paper, the Wilson-Thomas model is applied to predict the transition point for Bingham plastics. Laminar and turbulent friction losses are calculated to show that conditions at transition depend only on the Hedström number. The results are approximated by simplified fit functions. Comparison with existing empirical correlations and experimental data from various sources shows satisfactory agreement.

Il est souvent préférable d'utiliser les pipelines industriels transportant des matériaux non newtoniens près de la transition entre l'écoulement laminaire et l'écoulement turbulent. Pour le modèle classique des fluides de Bingham, la technique d'Hedström surestime les pertes de friction de l'écoulement turbulent parce qu'elle ne prend pas en compte l'épaississement de la couche visqueuse. Dans le présent article, on applique le modèle de Wilson-Thomas pour prédire le point de transition pour des fluides de Bingham. Les pertes de friction laminaires et turbulentes sont calculées et montrent que les conditions lors de la transition dépendent uniquement du nombre d'Hedström. Les résultats sont exprimés sous forme approximative par des fonctions de calage simplifiées. La comparaison avec des corrélations empiriques et des données expérimentales provenant de diverses sources montre un accord satisfaisant.

Keywords: non-Newtonian flow, turbulent flow, viscous-layer thickening, transition, pipelines

INTRODUCTION

The flow of non-Newtonian materials is of major commercial importance in many industries. In pipeline flow of such materials it is often desirable (for reasons of stability and economics) to operate near the transition from laminar to turbulent flow.

Over the decades, many formulas or "rheologic models" have been developed to represent non-Newtonian rheograms. It has been found that models with only two rheological parameters (one degree of complexity more than the basic Newtonian model) are of the greatest value from an engineering viewpoint. The most widely used in practice is the well-known Bingham or yield-plastic model, which is analyzed in the present paper.

For laminar flow in circular pipes, the analysis of the flow of a Bingham plastic is a classical case that has been known for decades; but turbulent flow, and the transition between the two types, has been more resistant to analysis. The early work of Hedström (1952), which will be considered below, is found to give estimates of turbulent friction gradient that are often much too conservative. Many subsequent workers have simply attempted to devise expressions for non-Newtonian Reynolds numbers or friction factors that could be substituted into equations for Newtonian pipe flow, rather than considering turbulent mechanisms.

The turbulent flow of Newtonian fluids in pipes is adequately understood for engineering purposes, although details may still be subject to uncertainty. In the simple models in common engineering use, the effect of viscosity is confined to a thin viscous sublayer near the pipe wall. Thus it is logical to expect that the main effect of non-Newtonian viscous parameters should also be in the sublayer. Making use of a suggestion made by Lumley (1973, 1978) to account for drag reduction caused by long-chain molecules, the authors of the present paper proposed some years ago that the viscous sublayer for non-Newtonian turbulent flows is generally thicker than for equivalent Newtonian flows and put forward a quantitative model to calculate this effect (Wilson and Thomas; 1985; Thomas and Wilson, 1987). This model has been widely cited in the textbook literature, including

* *Author to whom correspondence may be addressed.*
E-mail address: wilson@civil.queensu.ca

Shook and Roco (1991), Chhabra and Richardson (1999), and Wilson et al. (2006). An extended version of the model will be used below to analyze turbulent flow and the laminar-turbulent transition for pipeline flows of Bingham plastics.

LAMINAR FLOW OF NON-NEWTONIAN MATERIALS

For a plastic material, the rheogram does not pass through the origin, and no strain rate occurs until the shear stress exceeds some yield value. As noted above, the simple two-parameter model called the Bingham plastic is often employed to quantify this behaviour. Its rheogram is linear, passing through the Bingham yield stress τ_B at $du/dy = 0$ and having a slope η_B that is called "plastic viscosity," or "tangent viscosity," thus:

$$\tau = \tau_B + \eta_B\, du/dy \tag{1}$$

where u is local velocity and y is distance from the wall. This behaviour is shown schematically in Figure 1.

As shown on this figure, the viscosity μ, i.e., the ratio $\tau/(du/dy)$ represents the slope of a straight line passing through the origin. For a Bingham plastic, it is convenient to use a reduced stress variable θ, defined as τ/τ_B (for pipe flow $\theta = \tau_o/\tau_B$, where τ_o is the shear stress at the pipe wall). From the geometry of Figure 1, it is found that:

$$\mu = \eta_B\, \theta/(\theta - 1) \tag{2}$$

If the material being tested had been a Newtonian fluid, the rheogram would have been a straight line through the origin. As noted by Wilson and Thomas (1985), a measure of the departure from Newtonian behaviour is the area ratio α, i.e., the ratio of the stippled area beneath the rheogram of Figure 1 to the triangular area for a Newtonian fluid having the same value of τ. For a Bingham plastic this ratio is given in terms of θ by:

$$\alpha = (\theta + 1)/\theta \tag{3}$$

For the case of laminar flow in a circular pipe, the shear stress varies linearly from τ_o at the wall to zero at the centre line and, by Equation (2), μ can be found at any point in the flow. Integration gives the velocity at any location, and a further integration can be used to determine the discharge and hence the mean velocity V, as shown in any rheology text. The result is:

$$V = D\, \tau_o /(8\, \eta_B)[1 - 4/(3\theta) + 1/(3\theta^4)] \tag{4}$$

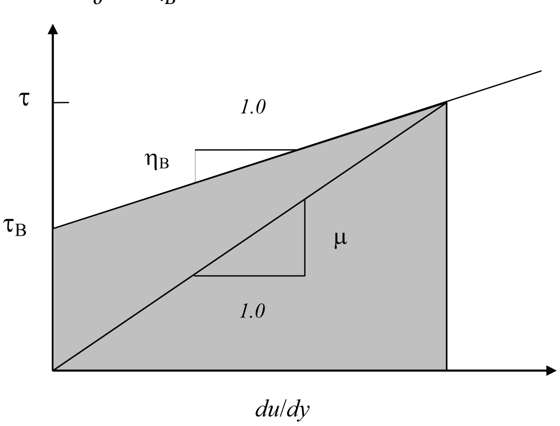

Figure 1. Schematic rheogram for Bingham plastic

At this point it is useful to introduce a dimensionless parameter developed by Hedström (1952)—the Hedström number He, defined as:

$$He = \rho\, \tau_B\, D^2/\eta_B^2 \tag{5}$$

The next step is to consider the ratio of V to the shear velocity U_*, which is equal to $\sqrt{[\tau_o/\rho]}$, or $\theta^{0.5}(\tau_B/\rho)^{0.5}$. For a Bingham plastic this ratio is given by Equation (4) as:

$$V/U_* = D\tau_B\theta\, \rho^{0.5}/(8\eta_B(\tau_B)^{0.5}\theta^{\,0.5})\, [1 - 4/(3\theta) + 1/(3\theta^4)] \tag{6}$$

Together with Equation (5), this expression simplifies to:

$$V/U_* = (He)^{0.5}\, \theta^{0.5}\, [1 - 4/(3\theta) + 1/(3\theta^4)]/8 \tag{7}$$

TURBULENT FLOW OF NON-NEWTONIAN MATERIALS

In order to understand and analyze non-Newtonian turbulent flow, some sort of flow model is required. One approach is to begin with the expression for the mean velocity of Newtonian turbulent flow in a smooth-walled pipe. For tests of turbulent flow of a non-Newtonian material, all quantities except μ will be available for each data point. Therefore, the equation can be solved for the viscosity in each case; the viscosity thus determined is called the equivalent turbulent-flow viscosity, and given the symbol μ_{eq}. The equation is then written:

$$V = 2.5\, U_*\, \ln(\rho\, D\, U_*/\mu_{eq}) \tag{8}$$

Substitution of the Hedström number (analogous to the derivation of Equation (7) gives the ratio V/U_* as:

$$V/U_* = 2.5\, \ln[(He)^{0.5}\theta^{\,0.5}(\eta_B/\mu_{eq})] \tag{9}$$

At this point a model must be developed for predicting μ_{eq} from the rheogram. An early model was that of Hedström (1952) who simply set μ_q equal to η_B. However, as demonstrated below, this model does not give good predictions for turbulent flow.

An adequate model of the turbulent flow of non-Newtonians must begin from Newtonian turbulent flow, which itself is a complex phenomenon. However, all that is usually required is a reasonable approximation to the velocity distribution. The model developed by the authors (Wilson and Thomas, 1985; Thomas and Wilson, 1987) was based on the simple 'engineering' profile in which the effect of fluid viscosity is confined to a thin sublayer which extends from the wall to a distance δ given by:

$$\delta \approx 11.6\, \mu/\rho\, U_* \tag{10}$$

where μ and ρ are the viscosity and density, respectively, of the Newtonian fluid and U_* is the shear velocity at the wall, as defined previously. Within the sublayer the velocity profile is taken to follow the linear relation, which incorporates the usual no-slip wall condition:

$$u = \tau_o y/\mu \qquad (y < \delta) \tag{11}$$

In the main flow it is assumed that all momentum transfer takes place by turbulent mixing, which is an inertial process rather than a viscous one. This gives rise to the well-known logarithmic velocity profile in this region. As the velocity gradient in the viscous sublayer is much steeper than that in the logarithmic zone, the sublayer has an influence on mean velocity which is disproportionate to its small thickness, and thus it is the sublayer that determines the influence of viscosity on the friction factor for Newtonian turbulent flow.

If a non-Newtonian fluid is to be substituted for the Newtonian one it is expected that in the logarithmic zone the momentum transport is still inertial in nature. The velocity gradient in this zone was not affected by Newtonian viscosity, and it would be expected that the same should apply for non-Newtonian rheological properties. (In the part of the flow nearest the pipe axis, some change in the velocity profile results from nonzero τ_B, and this will be incorporated below as a term denoted Ω.) Within the sublayer, which occupies such a small portion of the flow that variations in shear stress and velocity gradient are negligible, laminar conditions are approached. Here a linear velocity increase equivalent to Equation (11) should also apply for a non-Newtonian fluid.

Two questions arise at this point. The first concerns the value of μ that applies in Equations (10) and (11), and the second refers to the coefficient that specifies the thickness of the viscous sublayer (for Newtonian flows this is 11.6, as given in Equation (10), but the value is larger for non-Newtonians, as discussed below). The first question can be resolved noting that the "secant" slope μ is equivalent to the Newtonian viscosity in that it is the ratio of τ to du/dy. Thus, Equation (10) should still apply in principle for non-Newtonians, provided μ is understood in this sense and evaluated at $\tau = \tau_o$.

The remaining question concerns the thickness of the viscous sublayer. Wilson and Thomas (1985) proposed that this can be related to a conceptual model proposed by Lumley (1973, 1978) to explain the phenomenon of drag reduction in aqueous flows, wherein small quantities of certain long-chain molecules were added and a substantial reduction in frictional pressure drop was observed. These substances act to increase the size of the smallest, dissipative, turbulent eddies. Figure 2, which illustrates Lumley's model, graphs the distance from the wall, *y*, as the ordinate and representative eddy sizes as the abscissa. As indicated in the figure, the size of the large eddies (the macro-scale of turbulence) is directly proportional to the distance from the wall, while the size of the smallest eddies (the dissipative, or Kolmogorov, scale) does not change much with this distance.

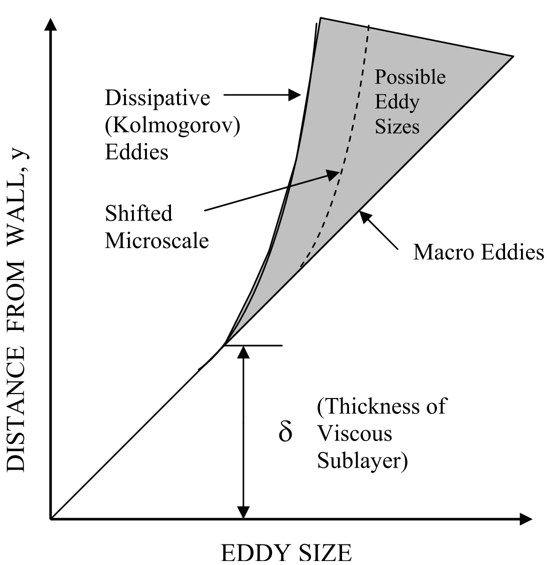

Figure 2. Eddy scales in turbulent flow (from Wilson and Thomas, 1985)

At large values of *y* the inertial macro-eddies are much bigger than the dissipative micro-eddies, and between them is a whole range of turbulent eddy sizes, shown shaded in Figure 2. As the wall is approached, the range of possible eddy sizes shrinks until the size of the largest and smallest eddies are equal, indicating the elimination of turbulence. At this point *y* equals δ, the thickness (in a statistical sense) of the viscous sublayer.

The dashed line of Figure 2 shows that increasing the size of the dissipative micro-eddies leads to an increase in the thickness of the viscous sublayer. It is known that the micro-eddy size is increased by long-chain molecules, and non-Newtonian rheological properties can produce a similar effect, as shown by Wilson (1989) and Wang and Larsen (1994). If other quantities are unaffected the thickened sublayer will, in turn, produce a higher mean velocity for the same wall shear stress, giving a lower friction factor.

In the predictive model for non-Newtonians developed by the authors (Wilson and Thomas, 1985; Thomas and Wilson, 1987) it was noted that the interaction of the eddies in turbulent flow causes them to increase in axial length, often very rapidly. This "vortex stretching" process produces abrupt increases in strain rates, and in the viscous dissipation of the smallest eddies. As the energy available for dissipation is fixed by the "turbulent energy cascade," the result is an increase in the micro-eddy size. The model uses the ratio of the integrals under the non-Newtonian and Newtonian rheograms—denoted by α, and defined above in connection with Figure 1—to estimate the size increase of the micro-eddies. From the relationship shown on the figure, it follows that the thickness of the sublayer should also be multiplied by a factor equal to α, while that of the superposed logarithmic layer is reduced by (α - 1). The result of these thickness changes is a displacement of the velocity profile beyond the sublayer. This displacement can be expressed formally by introducing an equivalent viscosity μ_{sl} into the well-known logarithmic velocity profile, giving:

$$u/U_* = 2.5 \ln(\rho y U_*/\mu_{sl}) + 5.5 \tag{12}$$

The evaluation of μ_{sl} is based on the combination of the thickened sublayer, proportional to $\mu\alpha$, and the reduced logarithmic layer, dependent on (α - 1). The result is:

$$\mu_{sl} = \mu\,\alpha\, e^{-4.64(\alpha-1)} \tag{13}$$

where the coefficient 4.64 represents the product of the sublayer coefficient of 11.6 and von Kármán's coefficient of 0.4. For a Bingham plastic, μ and α are given in terms of θ by Equations (2) and (3), and Equation (13) becomes:

$$\mu_{sl} = \eta_B[(\theta + 1)/(\theta - 1)]e^{-4.64/\theta} \tag{14}$$

Substitution of Equation (14) into Equation (9) gives the following expression for the ratio of V to U_* for turbulent flow of a Bingham plastic:

$$V/U_* = 2.5 \ln[(He)^{0.5}] + 2.5 \ln[\theta^{0.5}(\theta - 1)/(\theta + 1)] + 11.6/\theta - \Omega \tag{15}$$

The final term in Equation (15) takes account of any blunting of the velocity profile near the pipe centre line where $\tau < \tau_B$. As introduced by Wilson and Thomas (1985), Ω depends only on θ, and can be written:

$$\Omega = -2.5 \ln[(\theta - 1)/\theta] - 2.5(\theta + 0.5)/\theta^2 \tag{16}$$

Whether such blunting actually occurs remains a moot point, reference may be made to Xu et al. (1993).

It should also be noted that the V/U_* can be written $\sqrt{(8/f)}$ where f is the Darcy-Weisbach friction factor. Thus, f for a turbulent flow of a Bingham plastic can be determined directly from Equation (15) (with Equation (16) substituted in, if required). Values of f determined in this way are plotted in Figure 3 against Hedström's version of the Reynolds number (i.e. $\rho VD/\eta_B$). The parameters τ_B and η_B were evaluated to match a 7% kaolin slurry tested by Thomas (Wilson and Thomas, 1985) in the three pipe sizes noted. It is worth noting that the basic similarity of the results for the three pipes sizes studied supports the use of the no-wall-slip condition. This slurry had a rheogram that was very close to Bingham plastic behaviour. The figure also shows Thomas' data for these experiments, and the line of Hedström's hypothesis that $\mu_{eq} = \eta_B$.

Figure 3 illustrates several basic points. The first is the good general agreement between the values calculated from the model and the experimental data. In this regard, noteworthy agreement for various Bingham plastics has been found by other authors including Xu et al. (1993). The second point is that, for turbulent flow, both calculated and observed values of f fall significantly below the line of $\mu_{eq} = \eta_B$, indicating that μ_{eq}, and hence μ_{sl}, are substantially less than η_B. This finding implies that there is indeed a significant thickening of the sublayer for turbulent flows of Bingham plastics.

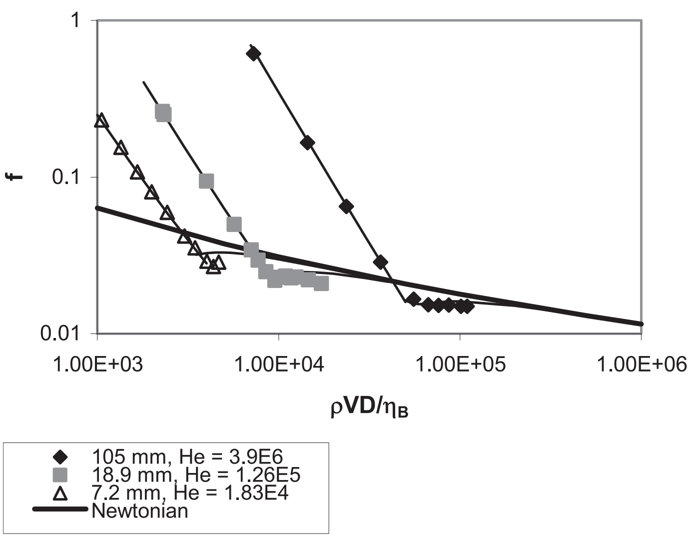

Figure 3. Logarithmic plot of f *versus* $\rho VD/\eta_B$

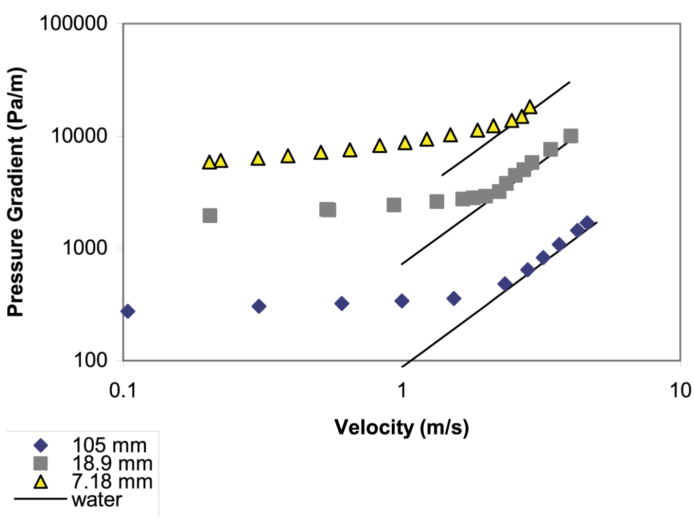

Figure 4. Logarithmic plot of pressure gradient *versus* V

A third point illustrated by Figure 3 is that the turbulent flow of a Bingham plastic tends to show remarkably small variations in f for large changes in flow velocity. In addition, this "plateau" value of f is smaller for the larger pipe, which follows from the present model as an effect of Hedström number. This behaviour of f is quite distinct from the wall-roughness effect shown on the Stanton-Moody diagram for Newtonian pipe flow, since the latter lies above the smooth pipe line, not below it.

REMARKS ON LAMINAR-TURBULENT TRANSITION

Figure 4 displays the kaolin data used for Figure 3, plotting both laminar and turbulent flow on a logarithmic graph of pressure gradient *versus* flow velocity V. The transitions shown in this figure are distinguished by a clear change of slope when the flow shifts from laminar to turbulent, marking a distinct intercept of the two individual curves.

This type of intercept is typically found when the material is strongly non-Newtonian (i.e., has a large value of the Hedström number). On the other hand, at sufficiently low Hedström numbers [below about 1700, as will be shown below] the behaviour begins to resemble that of a Newtonian fluid, where transition occurs when the Reynolds number $\rho VD/\mu_{eq}$ has a certain value, usually taken as $\rho V_T D/\mu_{eq} \approx 2100$. For this case, it is useful to know the friction factor, which is found, by iteration, to be $f_T \approx 0.049$, equivalent to $V_T/U_* = 12.76$. The latter value can be substituted directly into the left-hand side of Equation (15) to obtain the required condition in terms of He and θ. For engineering purposes, it is generally more convenient to use the Hedström-type Reynolds number $\rho V_T D/\eta_B$, and on this basis the transition condition for low Hedström numbers can be closely approximated by the fit equation:

$$\rho V_T D/\eta_B = 2100/\{1.0 + 8.3(10^{-8})[\mathrm{Log}_{10}(\mathrm{He})]^{13}\} \quad [\mathrm{He} < 1700] \quad (17)$$

For cases like those described by Figure 4, typical of higher Hedström numbers, the laminar-turbulent intercept can be obtained by equating Equations (7) and (15), which have a common left-hand side, a single parameter He, and a variable θ. First, He is set to a series of values and then, for each one, θ is varied until the desired equality is achieved. This value of θ can then be substituted back into the equations to obtain V_T/U_*, where V_T is the flow velocity at transition. As shown below, this in turn gives the friction factor at transition, f_T, and the ratios $\rho V_T D/\eta_B$ and $V_T/[(\tau_B/\rho)^{0.5}]$, the last of which is also denoted by V_{Trel}. Comparison with experimental results will be presented in the following section.

ANALYTIC MODEL AND ITS OUTPUT

The basic relationships for the present analytic model of laminar-turbulent transition for pipeline flow of Bingham plastics have been presented in the previous sections as Equations (7) and (15) (with the substitution of Equation (16)) plus the condition for $\rho VD/\mu_{eq} = 2100$ (given by Equation (17)). As noted, the left-hand side of Equations (7) and (15) equals $\sqrt{(8/f)}$, and hence the solution of these equations can be reduced to a plot of f at transition (f_T) as a function of Hedström number He. This plot is shown as Figure 5. As noted above, the condition that $\rho VD/\mu_{eq} \approx 2100$ is equivalent to f of 0.049. This forms an upper limit to f_T in Figure 5, applying to all values of He < 1700.

An alternative method of plotting the result of the model is shown in Figure 6, which also has the Hedström number on the abscissa, but has on the ordinate the ratio $\rho V_T D/\eta_B$, which is equal to the product $[V_T/U_*](He)^{0.5}\theta^{0.5}$, and can readily be calculated from the output of the model. For He > 10^5, the model output is virtually identical to the equation:

$$\rho V_T D/\eta_B = 25(He)^{0.50} \qquad [He > 10^5] \qquad (18)$$

In the intermediate range between the applicability of Equations (17) and (18), the output of the model can be approximated by the equation:

$$\rho V_T D/\eta_B = 80(He)^{0.40} \qquad [1700 < He < 10^5] \qquad (19)$$

The next step is to compare the lines of Figure 6 to available experimental data. First, however, it is worth stressing that experimental data have not been used in deriving the lines on Figure 6, which represent the predictions of the Wilson-Thomas model based on sublayer thickening. (The solid lines are the model predictions and the dotted lines are the approximating functions.)

The corpus of data which is plotted as Figure 7 (using the same axes as Figure 6) comes from many sources. For the points marked "loam clay," "kaolin," "magnetite concentrate," "minus 1 mm coal" and "clay + fine sand," see Thomas (1978). For the zinc concentrate see Weston et al. (1978), and for the silica flour see Tuft (1978). Wasp (2005) is a personal communication and the publications by Kenchington (1978) and Kazanskij et al. (1978) are listed in the References below.

A particularly useful way of displaying the model output and the data is shown as Figure 8, which again uses the logarithm of He on the abscissa, but now has as ordinate $V_T/[(\tau_B/\rho)^{0.5}]$. The latter quantity, called the relative transition velocity V_{Trel}, equals

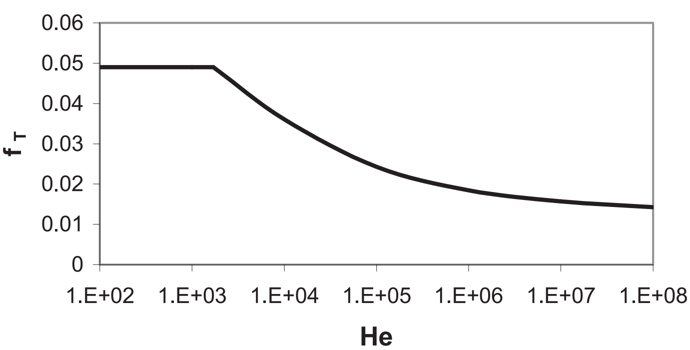

Figure 5. Logarithmic plot of f_T *versus* He

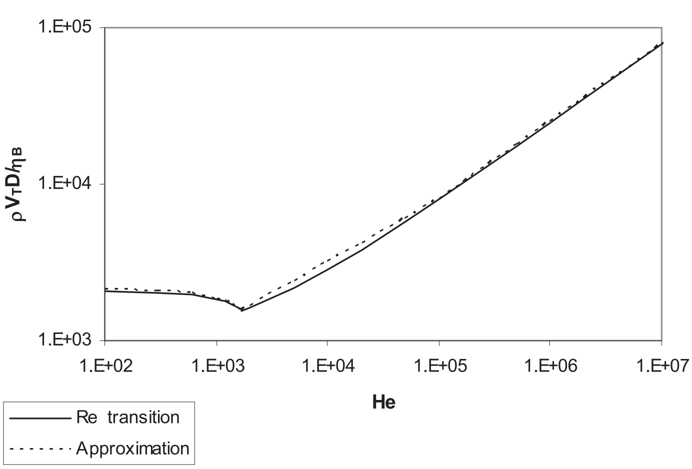

Figure 6. Logarithmic plot of $\rho V_T D/\eta_B$ *versus* He, showing correlations and fit lines

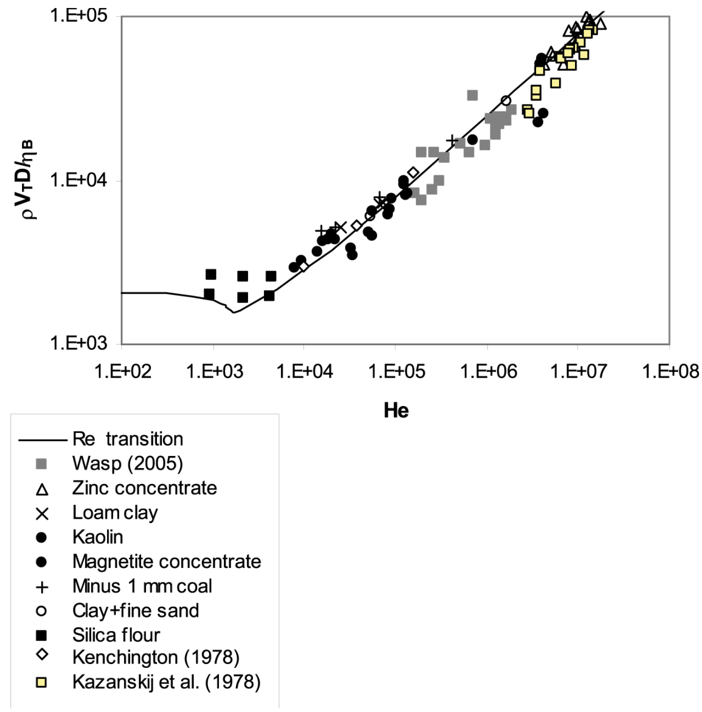

Figure 7. Logarithmic plot of $\rho V_T D/\eta_B$ *versus* He, showing data

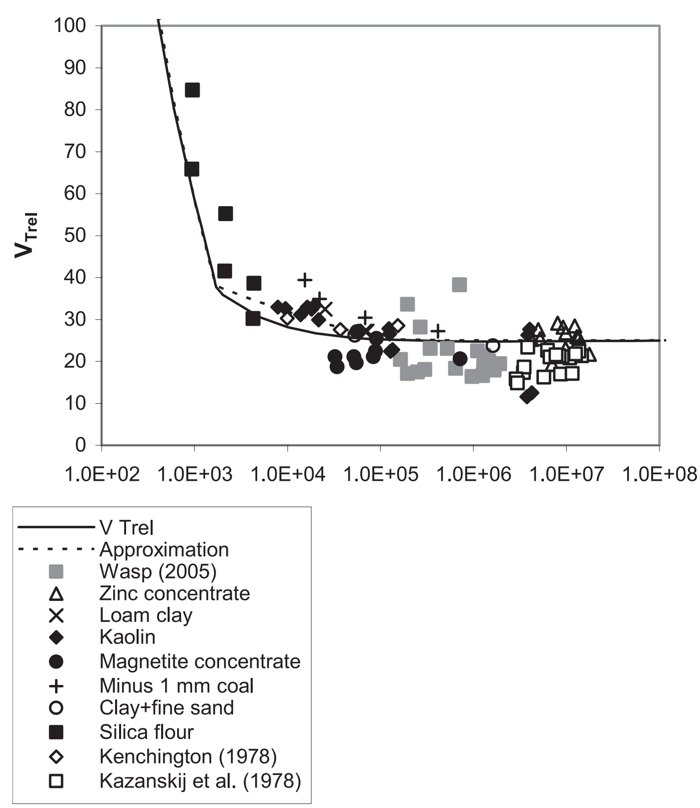

Figure 8. Plot of V_{Trel} *versus* Log(He)

$[V_T/U_*]\theta^{0.5}$ and again can readily be calculated from the model output. For values of He between 1700 and 10^5, V_{Trel} can be approximated by $80(He)^{-0.10}$ (equivalent to Equation (19)).

It is particularly noteworthy that for all values of He greater than about 10^5 the relative transition velocity is effectively equal to a constant value, predicted by the Wilson-Thomas model to be 25, i.e.;

$$V_T/(\tau_B/\rho)^{0.5} = 25 \qquad [He \geq 10^5] \qquad (20)$$

Comparison may be made with correlations developed by other workers. One of the best-known is that of Thomas (1963), which is equivalent to a quadratic equation linking $\rho V_T D/\eta_B$ and He. As shown elsewhere (Wilson et al. 2006, p. 75), this predicts a value of $V_T/(\tau_B/\rho)^{0.5} = 30$ at He = 10^4, dropping to 19 at He ≥ 10^8. Another early proposal was that of Hanks (1963).

Although references to this proposal are still found in the literature, it was shown by Govier and Aziz (1972), Venton (1982) and Wilson and Thomas (1985) that Hanks' proposed transition velocity seriously under-predicts experimental determinations. Later, Malin (1997) applied both k-ε and k-ω modelling to turbulent pipe flow of Bingham plastics. His analysis correctly predicts that the laminar line for f passes through the Hedström line and then drops below it (like the behaviour shown in Figure 3). However, it has the turbulent line snapping back to the Hedström line at higher He; thus failing to duplicate the plateau in f which is observed experimentally (and predicted by the present model). In this instance, it appears that the more complex turbulent models have not yet matched that of simple sublayer thickening.

A more recent publication, that of Slatter and Wasp (2000), is based directly on the correlation of experimental points, using straight fit lines on a logarithmic plot of $\rho V_T D/\eta_B$ *versus* He. For the range $1.7 \times 10^3 < He < 1.5 \times 10^5$, their result is equivalent to $\rho V_T D/\eta_B = 155\ He^{0.35}$ (which plots rather near Equation (19) above), and for $He > 1.5 \times 10^5$ they obtained $V_T/(\tau_B/\rho)^{0.5} = 26$ (which is remarkably close to Equation (20)).

CONCLUSION

Non-Newtonian pipeline flows are of importance in many industries, and for reasons of stability and economics it is often desirable to operate near the laminar-turbulent transition. Although the laminar side of the transition was solved decades ago, the turbulent side has been less well understood. For the commonly-used two-parameter Bingham plastic model, the old Hedström technique overestimates friction losses. The authors of the present paper showed that this occurs because the Hedström model does not take account of viscous-layer thickening.

The Wilson-Thomas model, which does account for viscous-layer thickening, has now been applied to the prediction of the transition point for Bingham plastics. Laminar and turbulent friction losses are expressed in terms of common parameters and variables, and equated at the transition point. On iterating to eliminate the stress ratio, it is found that the conditions at transition depend only on the Hedström number. The calculated relationships have been approximated by simplified fit functions valid over specific ranges, and compared to existing empirical correlations and to experimental data from various sources, with satisfactory results.

It is of particular interest that for $He > 10^5$ the dimensionless transition velocity V_{Trel} predicted by the authors' model has a constant value, equal to 25.

NOMENCLATURE

D	internal pipe diameter (m)
f	friction factor (Darcy-Weisbach) (-)
f_T	value of f at laminar-turbulent transition (-)
He	Hedström number (see Equation (5)) (-)
u	local velocity at distance y from wall (m/s)
U_*	shear velocity ($\sqrt{[\tau_o/\rho]}$) (m/s)
V	mean (flow) velocity (m/s)
V_T	value of V at laminar-turbulent transition (m/s)
V_{Trel}	relative transition velocity $V_T/(\tau_B/\rho)^{0.5}$ (-)
y	distance from pipe wall (m)

Greek Symbols

α	area ratio of rheogram (-)
δ	thickness of viscous sublayer (m)
η_B	Bingham plastic (tangent) viscosity (Pa.s)
θ	shear stress ratio τ_o/τ_B (-)
μ	secant viscosity (Pa.s)
μ_{eq}	equivalent viscosity for turbulent flow (see Equation (8)) (Pa.s)
μ_{sl}	equivalent viscosity for viscous sublayer (see Equation (13)) (Pa.s)
ρ	density of material (kg/m^3)
τ	shear stress (Pa)
τ_B	Bingham (yield) shear stress (Pa)
τ_o	shear stress at pipe wall (Pa)
Ω	effect of τ_B on velocity-profile blunting (see Equation (16))

REFERENCES

Chhabra, R. P. and J. F. Richardson, "Non-Newtonian Flow in the Process Industries," Butterworth-Heinemann, Oxford, U.K. (1999).

Govier, G. W. and K. Aziz, "The Flow of Complex Mixtures in Pipes," Van Nostrand Reinhold, New York, NY, U.S. (1972)

Hanks, R. W., "The Laminar-Turbulent Transition for Fluids with a Yield Stress," AIChE J. 9(3), 306–309 (1963).

Hedström, B. O. A., "Flow of Plastics Materials in Pipes," Ind. Eng. Chem. **44**(3), 651–656 (1952).

Kazanskij, I., H. J. Mathias and K. Luck, "Behaviour of Pseudoplastic Slurries in Pipe Flow," Proc. Hydrotransport *5*, BHR Group Ltd., Cranfield, Bedford, U.K. (1978), pp. C3-35–C3-48.

Kenchington, J. M., "Prediction of Pressure Gradient in Dense Phase Conveying," Proc. Hydrotransport 5, BHR Group Ltd., Cranfield, Bedford, U.K. (1978), pp. D7-91–D7-102.

Lumley, J. L., "Drag Reduction in Turbulent Flow by Polymer Additives," J. Macromol. Sci., Polym. Rev. 7, 263–290 (1973).

Lumley, J. L., "Two-Phase Flow and Non-Newtonian Flow," in Turbulence, P. Bradshaw, Ed., Topics in Applied Physics, Vol. 12, Springer-Verlag, Berlin, Chap. 7 (1978).

Malin, M. R., "The Turbulent Flow of Bingham Plastic Fluids in Smooth Circular Pipes," Int. J. Heat Mass Transfe **24**(6), 793–804 (1997).

Shook, C. A. and M. C. Roco, "Slurry Flow Principles and Practice," Butterworth-Heinemann, Boston, MA, U.S. (1991).

Slatter, P. T. and E. J. Wasp, "The Laminar/Turbulent Transition in Large Pipes," Proc. 10th Int. Conf. on Transport and Sedimentation of Solid Particles, AUV, Wrocław, Poland (2000), pp. 389–399.

Thomas, A. D., Previously unpublished data. By permission C. H. Warman Group, Sydney, Australia (1978).
Thomas, A. D., "Slurry Pipeline Rheology," Proc. 2nd Nat'l Conf. on Rheology, Sydney, Australia (1981).
Thomas, A. D. and K. C. Wilson, "New Analysis of Non-Newtonian Turbulent Flow—Yield Power-Law Fluids," Can. J. Chem. Eng. **65**, 335–338 (1987).
Thomas, D. G., "Non-Newtonian Suspensions. Part 1 Physical Properties and Laminar Transport Characteristics," Ind. Eng. Chem. **55**(11), 18–29 (1963).
Tuft, P., Previously unpublished data. By permission C. H. Warman Group, Sydney, Australia (1978).
Venton, P. B., "The Gladstone Limestone Pipeline," Proc. Hydrotransport 8, BHR Group Ltd., Cranfield, Bedford, U.K. (1982), pp 49–62.
Wang, Z. and P. Larsen, "Turbulent Structure of Water and Clay Suspensions with Bed Load," J. Hydraulic Eng. ASCE **120**(5), 577–600 (1994).
Wasp, E. J., Private communication (2005).
Weston, M., R. Gandhi and A. D. Thomas, "Test Loop Data for Zinc Concentrate," By permission Zinifex Century Mine, Queensland, Australia (2002).
Wilson, K. C., "Transitional and Turbulent Flows of Bingham Plastics," Miner. Process. Extr. Metall. Rev. 20, 225–237 (1999).
Wilson, K. C. and A. D. Thomas, "A New Analysis of the Turbulent Flow of Non-Newtonian Fluids," Can. J. Chem. Eng. **63**, 539–546 (1985).
Wilson, K. C., "Two Mechanisms for Drag Reduction," Drag Reduction in Fluid Flows, Techniques for Friction Control, H. R. J. Sellin and R. T. Moses, Eds., Ellis Horwood Ltd., Chichester, U.K. (1989), pp. 1–8.
Wilson, K. C., G. R. Addie, A. Sellgren and R. Clift, "Slurry Transport Using Centrifugal Pumps," 3rd ed., Springer, Norwell, MA, U.S. (2006)
Xu, J., R. Gillies, M. Small and C. A. Shook, "Laminar and Turbulent Flow of kaolin Slurries," Proc. Hydrotransport 12, BHR Group Ltd., Cranfield, Bedford, U.K. (1993), pp. 595–613.

Manuscript received November 25, 2005; revised manuscript received February 9, 2006; accepted for publication February 9, 2006.